Diseases of the Female Pelvis
Advances in Imaging Evaluation

Alice C. Brandão, MD[a,b,*], Anelise Oliveira Silva, MD[a,b,c]

KEYWORDS

• MRI • Female pelvic MRI • Diffusion • Perfusion • Functional pelvic MRI

KEY POINTS

- Magnetic resonance (MR) has been widely accepted as a powerful imaging modality for the evaluation of the pelvis because of its intrinsic superior soft tissue contrast compared with other imaging modalities.
- MR imaging is mainly used for staging of uterine cancers and as a problem-solving modality in patients with ultrasonographically indeterminate masses.
- MR imaging provides multiplanar imaging of the zonal pelvic anatomy, mainly through high-resolution T2-weighted images.
- Functional study with perfusion and diffusion allows the evaluation of microvascular characteristics and cellularity of the lesions.
- Functional evaluation favors the differentiation of benign from malignant lesions.

INTRODUCTION

Magnetic resonance (MR) has been widely accepted as a powerful imaging modality for the evaluation of the pelvis because of its intrinsic superior soft tissue contrast compared with that of computed tomography (CT).[1]

At this moment, MR imaging is mainly used for staging of uterine cancers, and as a problem-solving modality in patients with ultrasonographically indeterminate masses.

At our site, characterization of congenital female pelvic anomalies, diagnosis of adenomyosis, planning of appropriate treatment for benign myometrium diseases, and endometriosis staging are other common clinical applications for MR imaging of the pelvis.

CT is applied for staging purposes in patients with ovarian, bladder, and prostate cancer, whereas MR imaging is the method of choice for local staging of uterine cancer, allowing detection of infiltration of neighboring structures.[1]

MR imaging does not use ionizing radiation, which is particularly important in the evaluation of young women and represents another advantage over CT.

The main goals of female pelvic MR imaging include (1) multiplanar display of the zonal pelvic anatomy, mainly with high-resolution T2-weighted images; (2) detection and characterization of diffuse and focal lesions; (3) detection and characterization of congenital female pelvic anomalies; and (4) follow-up of disease processes.[2]

Despite the high sensitivity of conventional MR imaging for the assessment of most pelvic lesions, in certain cases, such as peritoneal lesions, lymph node staging, and assessment of therapeutic response of some tumors, the morphologic information provided by MR imaging may be insufficient. The functional evaluation provided by perfusion

Disclosures: None.
Funding Sources: None.
[a] IRM, Ressonância Magnética, Rio de Janeiro, Brazil; [b] Department of Radiology, Clínica Felippe Mattoso, Avenida das Americas 700, 319, Rio de Janeiro 30112011, Brazil; [c] Department of Radiology, Hospital Federal da Lagoa, Rio de Janeiro, Brazil
* Corresponding author.
E-mail address: brandaosalomao@gmail.com

Magn Reson Imaging Clin N Am 21 (2013) 447–469
http://dx.doi.org/10.1016/j.mric.2013.01.003
1064-9689/13/$ – see front matter

and diffusion studies, which allow estimation of the microvascular characteristics and cellularity of the lesions, favors the differentiation of benign from malignant lesions.[3]

IMAGING TECHNIQUE

Standard MR Protocol

Our standard MR protocol includes axial, sagittal, and coronal T2-weighted fast spin-echo images, axial T1-weighted gradient-echo images with and without fat suppression, and sagittal T1-weighted gradient-echo with fat suppression. Sagittal and axial images are acquired before and after the intravenous injection of a gadolinium-based contrast material.

MR imaging is performed in a 1.5-T unit (Signa; GE Medical Systems, Milwaukee, WI), with a phased-array coil, which is used to improve signal-to-noise ratio.

Four to 6 hours of fasting before the examination is recommended.

It is also important to empty the bladder before the examination.

Routinely, to reduce intestinal peristalsis and uterine contractions, 10 mg of butyl scopolamine (Buscopan; Boehringer Ingelheim, Ingelheim, Germany) is injected intravenously.

For congenital female pelvic anomalies, endometriosis, and uterine carcinoma staging, to distend the vaginal fornix, 20 mL of gel is infused into the vagina.

For endometriosis, additional bowel preparation is recommended, using glycerin suppository 2 hours before the examination and 80 mL of saline solution rectally (**Fig. 1**).

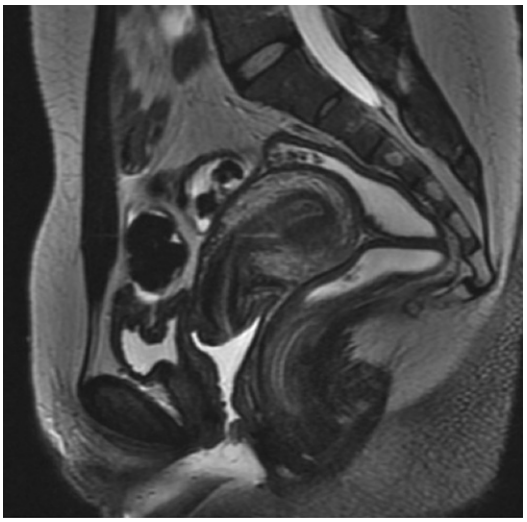

Fig. 1. T2-weighted image. Sagittal plane. Vaginal fornix distended by gel and rectum distended by saline solution.

Functional Sequences

Diffusion-weighted imaging

Diffusion-weighted imaging (DWI) is an MR technique that depicts molecular diffusion, which is the Brownian motion of water protons in biologic tissues.[1]

In the pelvis, DWI is most commonly acquired in the axial plane, as the magnetic field strength is more homogeneous close to the isocenter of the magnet, especially along the cranio-caudal direction, which leads to less susceptibility-induced signal loss and distortions in the axial images, compared with single-oblique and double-oblique acquisitions (**Fig. 2**).[1]

However, for endometrial carcinoma staging, we acquire the coronal oblique plane perpendicular to the uterine cavity. This sequence improves the accuracy of myometrium invasion identification (**Fig. 3**).

To obtain good-quality multiplanar reconstructions, the section thickness should be reduced to about 3 mm or less. If necessary, additional signal averaging might be indicated to ensure an adequate signal- to-noise ratio (SNR).

Diffusion-weighted images (DWIs) are usually acquired before contrast agent administration, although it has not yet been proved that this is required in all situations (**Table 1**).[1]

Choosing the b values for the DWI acquisition is not always straightforward. The largest b value used in the sequence defines the echo time of the sequence, and higher maximal b values (and subsequently longer echo times) yield greatly reduced SNR in the resulting images.

Because the b value is the strength of the diffusion sensitizing gradient, at a b value of 0 s/mm^2 (no diffusion sensitizing gradient), free water molecules have high signal intensity (SI), the SI being based on T2 weighting.

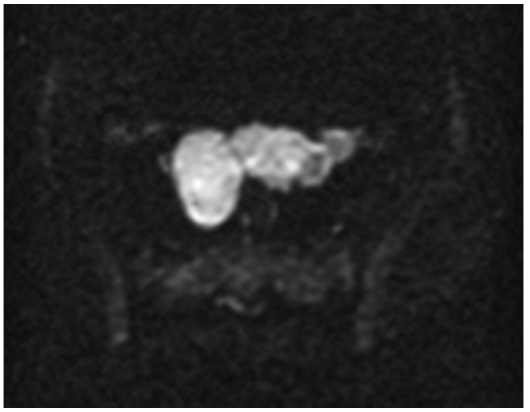

Fig. 2. DWI. Axial plane. Endometrium carcinoma staging. Note adnexal bilateral invasion presenting with high SI.

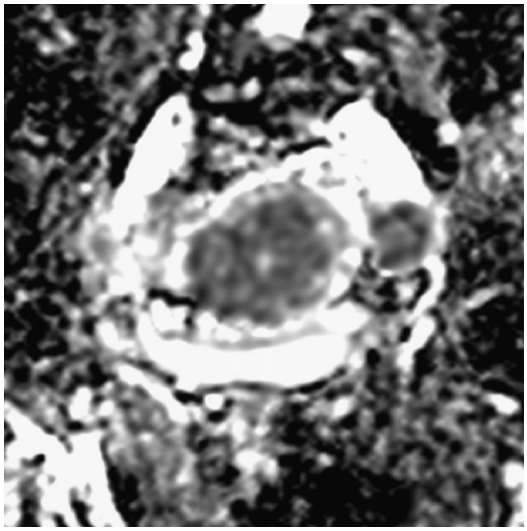

Fig. 3. DWI. Coronal oblique plane, perpendicular to the uterine cavity. Endometrium carcinoma staging. Note diffuse myometrium invasion.

By using mainly low b values, the apparent diffusion coefficient (ADC) that is calculated will be higher and reflects a combination of both perfusion and diffusion effects, whereas by using only higher b values (0.100 s/mm^2), the resulting ADC values will be much lower and better approximate the true diffusion of the tissue.[1,4,5]

Studies in the literature report different choices of maximal b values, usually of 500 to 1000 s/mm^2. Currently used clinical MR systems should, in most cases, be capable of obtaining good-quality DWIs with a maximal b values of 1000 s/mm^2. A range of intermediate b values can be selected depending on the type of quantitative analysis anticipated. Minimally, only 2 b values (most often b = 0 and 1000 s/mm^2) are required to calculate the ADC, expressed in square millimeters per second, if a monoexponential fit is used, by using the following equation: S = S0 exp (2b ADC), where S is the SI after application of the diffusion gradient, S0 is the estimated SI at b value of 0 s/mm^2, and b is strength of the applied diffusion-sensitizing gradients. However, application of more b values is usually recommended.[1]

The radiologist should be aware of the choice of b values to correctly interpret the resulting ADC values. We obtain DWIs with maximal b values of 1000 s/mm^2 with adequate SNR.

Qualitative analysis DWI is performed with at least 2 b values, including a b value of 0 s/mm^2 and a higher b value of 500 to 1000 s/mm^2.

The signal decay in tissues at different b values is generally biexponential.[6] The initial component of signal decay is signal loss caused by flowing blood (fast-moving water molecules will dephase but will not readily rephase and will loose signal even with small b values). The second component is due to the movement of water in the intracellular and extracellular spaces. A region of high signal intensity at high b-value DWI suggests restricted diffusion consistent with highly cellular tissue (tightly packed water molecules may readily be rephased by the rephasing gradient). The signal loss in water molecules at different b values can be used for lesion detection or characterization (**Fig. 4**).[6]

Quantitative analysis: ADC value The ADC represents the slope (gradient) of a line that is produced when the logarithm of relative signal intensity of tissue is plotted along the y-axis versus b values along the x-axis, thereby linearizing the exponential decay function. Quantitative analysis of DWI findings can be performed only if at least 2 b values are used for imaging. The optimal b values for tissue characterization depend on the tissue (organ) being evaluated.[6]

ADC values are related to the proportion of extracellular and intracellular components within the tissue. Increased tissue cellularity or cell density decreases the ADC measurement. Thus, high ADCs suggest benign processes with low cellularity, whereas low ADCs might indicate malignancy with large cell diameter and higher cell density, which restricts water diffusion. Therefore, ADC measurements can be valuable in differentiating benign from malignant lesions (**Fig. 5**).[4]

Dynamic Contrast-Enhanced–MR Imaging

Angiogenesis plays a vital role in the growth and spread of tumors. It means the sprouting of new capillaries from existing blood vessels, and, along with the vasculogenesis, the generation of new

Table 1
Transverse diffusion-weighted imaging parameters in our institution

TE	TR	FOV	Slice	Space	Matrix	NEX	Direction Frequency	Diffusion Direction	b Value	Pulse Sequence
Minimum	5675	40	3.0 mm	0.5	128 × 192	16	R-L	Slice	1000 mm^2/s	Spin-echo

Abbreviations: FOV, field of view; R-L, right to left; TE, echo time; TR, repetition time.

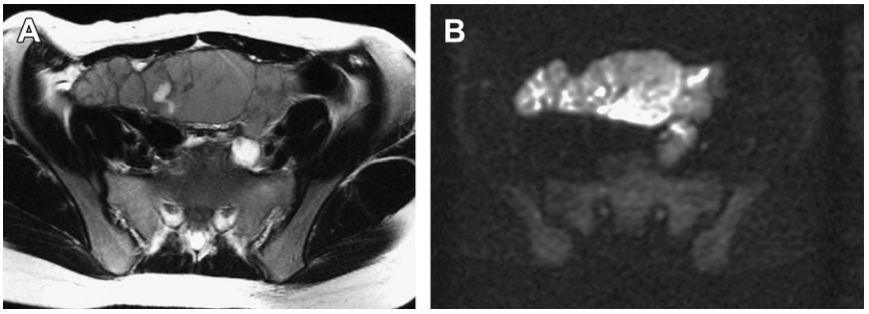

Fig. 4. Bilateral ovary mucinous adenocarcinoma. (*A*) T2-weighted image. Axial plane. (*B*) Axial plane DWI. High-SI ovaries and peritoneal lesions suggest restricted diffusion.

blood vessels, are the 2 primary methods of vascular expansion by which nutrient supply to tumor tissue is adjusted to match physiologic needs.[7]

Dynamic contrast-enhanced (DCE)-MR imaging is a noninvasive method that allows evaluation tumor angiogenesis. The findings are related to differences in microvascular characteristics observed in normal and malignant tissues. There are some features considered characteristic of malignant vasculature, which can be evaluated by DCE-MR imaging, such as poorly formed fragile vessels with high permeability to macromolecules, arteriovenous shunt, and extreme heterogeneity of vascular density.[8]

DCE-MR enables qualitative and quantitative assessment of tumor status. Insights into these physiologic processes are obtained qualitatively by characterizing kinetic enhancement curves or quantitatively by applying complex compartmental modeling techniques (**Fig. 6**).

DCE-MR imaging includes a DCE T1-weighted gradient-echo sequence, acquired before, during, and after a bolus injection of a low-molecular-weight contrast agent, gadolinium. As the agent enters into a tissue, it changes the MR signal intensity of the tissue. As the contrast agent flows out of the tissue, the MR signal intensity returns to its baseline value.

Serial images must be acquired with sufficient temporal resolution to demonstrate the enhancement characteristics of the tumor being investigated, but at the same time with enough spatial resolution so that the inherent heterogeneity of the lesion can be adequately probed. Most studies use temporal resolution in the 10-second to 30-second range. High spatial resolution is typically selected if a "semiquantitative" analysis is planned, whereas the high temporal resolution approach is selected if a full quantitative analysis is planned.[9]

Semiqualitative analysis

Semiquantitative evaluation of the DCE-MR images is based on SI changes that can be evaluated using (1) the SI curve, (2) the slope and height of the enhancement curve (time-to-peak), (3) maximum SI (peak enhancement), and (4) wash-in/washout gradient.

The technique used is a multiphase DCE T1-weighted fat-suppressed sequence obtained before intravenous administration of gadolinium-based contrast material and 0, 30, 60, 90, and

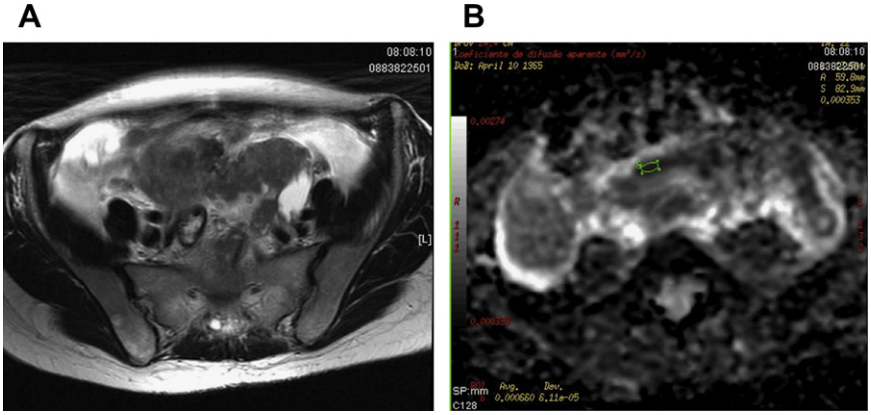

Fig. 5. Peritoneal implants. (*A*) T2-weighted image. Axial plane. (*B*) ADC map. Axial plane. Low-SI peritoneal lesions (ADC value – 0,6), suggest restricted diffusion.

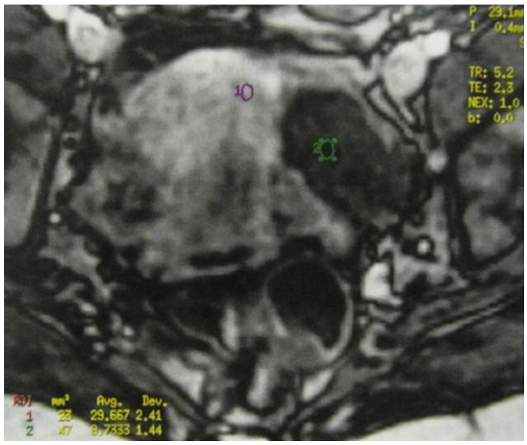

Fig. 6. Left adnexal mass. Fibrotecoma. DCE-MR imaging. DCE T1-weighted gradient-echo sequence acquired before, during, and after the bolus injection of gadolinium. As the agent enters into a tissue, it changes the MR SI of the tissue.

120 seconds after injection. The entire mass is included in the 5-point dynamic run acquisition. With standard breast MR software on a commercially available MR imaging workstation, a region of interest (ROI) is manually drawn over the most avidly enhancing solid component of the lesion, and the SI at each time point is recorded. For each ROI, enhancement parameters are automatically calculated and displayed as both numerals and SI versus time curves. These parameters include tissue SI on unenhanced T1-weighted images (SI0); SI at maximum absolute contrast enhancement (SImax); maximum relative SI (SIrel), which is relative to SI0 (SIrel = [SImax− SI0]/[SI0 × 100]); and wash-in rate (WIR), the difference between SI0 and SImax divided by time (in seconds).[10]

Another semiquantitative DCE-MR imaging technique involves rapid acquisition of DCE-MR images every 5 seconds for 2 to 4 minutes after injection of contrast material with a limited (1.5-cm) section that covers the solid portion of the mass, usually an adnexal lesion, which will be compared with the adjacent myometrium. The high temporal resolution of this DCE-MR imaging technique allows derivation of accurate time-intensity curves and other early enhancement parameters with an MR imaging workstation and additional computer software; however, the spatial resolution is lower (**Fig. 7**).[11]

This evaluation has the obvious advantage of being very straightforward to implement and can be performed in near real-time. The limitation is that the parameters do not necessarily have clear physical correlates because they are "mixed" measures. This approach has been particularly successful for breast and adnexal lesions.[9]

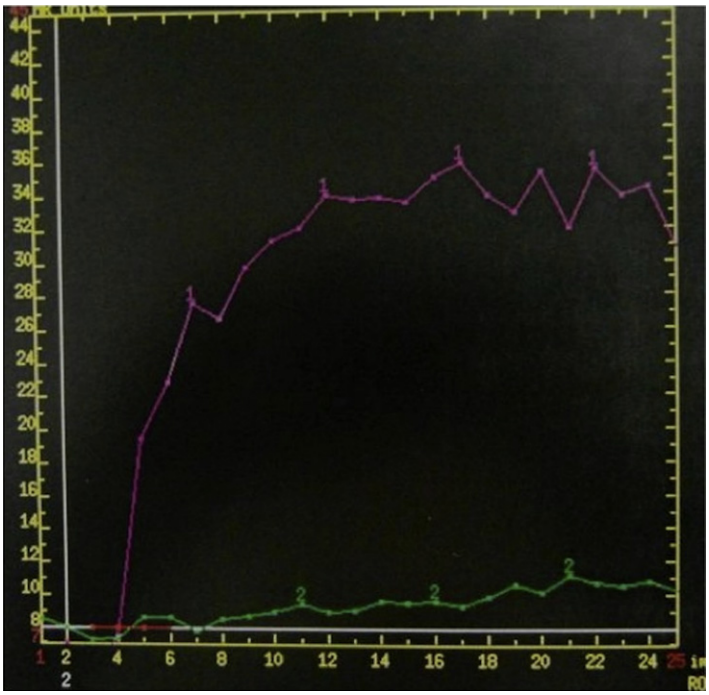

Fig. 7. Same case as **Fig. 6.** The high temporal resolution of this DCE-MR imaging technique allows derivation of accurate time-intensity curves.

Quantitative analysis

DCE-MR imaging is a noninvasive technique that allows measurement of the density, integrity, and leakiness of tissue vasculature. By analyzing the associated SI time course using an appropriate mathematical model, physiologic parameters related to blood flow, vessel permeability, and tissue volume fractions can be extracted for each voxel or ROI.

In the quantitative approach, a pharmacokinetic model is applied to changes in the contrast agent concentrations in tissue, and quantitative kinetic parameters are derived. They include (1) transfer constant of the contrast agent (Ktrans), (2) rate constant (Kep), and (3) interstitial extravascular extracellular space (Ve). The quantitative approach can be quite complex to implement.[12]

DCE-MR imaging related to pelvic organs

To design a DCE-MR imaging protocol, it is important to consider the goals of the study and carefully select the appropriate parameters balancing the needs of the study with resolution issues.

Uterus For uterus lesion characterization, the DCE-MR imaging consists of a sequentially ordered 3-dimensional T1-weighted fast-spoiled gradient-recalled echo of 4 contiguous sagittal sections. The bolus injection of gadopentetate dimeglumine (0.1 mmol/kg at a rate of 2 mL/s) is given 30 seconds after the beginning of acquisition and is immediately followed by a flush of 10 mL of normal saline at the same rate. The arterial phase is found at 18 seconds, based on the enhancement curves. The other 2 time points for the subtraction study are chosen by adding 60 seconds (portal venous phase) and 120 seconds (equilibrium phase) to the arterial phase (**Fig. 8**, **Table 2**).[13–17]

Adnexa For adnexal lesion characterization, DCE-MR imaging is acquired as a free-breathing axial DCE non–fat-suppressed T1-weighted gradient-echo 3-dimensional sequence. Images are obtained at 2.4-second intervals, beginning 5 seconds before the bolus injection and continuing for 320 seconds after the injection. The study must include the solid components of the ovarian tumor seen on the T2-weighted images as well as the uterus. Using a power injector at a rate of 2 mL/s, 0.1-mmol/kg of gadolinium contrast is given intravenously followed by 10 mL of normal saline to flush the tubing (**Table 3**).

A 3-dimensional FIESTA (fast imaging employing steady-state acquisition) sequence is acquired with similar parameters, being useful for the imaging analysis. The ROIs are placed within the solid tissue and normal outer myometrium selected on precontrast FIESTA images (**Fig. 9**).

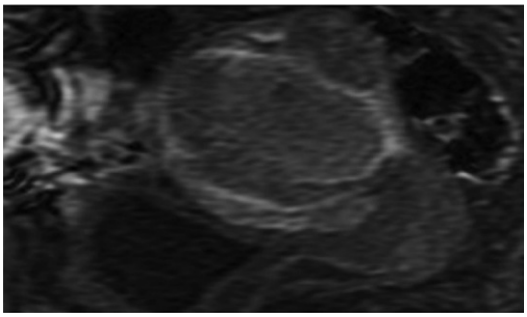

Fig. 8. Endometrial carcinoma with outer half myometrium invasion. DCE-MR imaging. Three-dimensional T1-weighted fast-spoiled gradient-recalled sagittal section.

ADVANCES IN UTERUS IMAGING

Endometrium

Endometrial carcinoma

The most common gynecologic malignancy, endometrial carcinoma, typically occurs in postmenopausal women, and presents with abnormal bleeding. Most endometrial malignancies are adenocarcinomas, which account for 90% of endometrial neoplasms.

Adenocarcinoma with squamous differentiation, adenosquamous carcinoma, clear-cell carcinoma, and papillary serous carcinoma represent less common histologic types. Clear-cell carcinoma and papillary serous carcinoma carry a worse prognosis.[18,19]

Depth of myometrial invasion is the most important morphologic prognostic factor, correlating with tumor grade, presence of lymph node metastases, and overall patient survival. The prevalence of lymph node metastases increases from 3% with superficial myometrial invasion to 46% with deep myometrial invasion.[20–22]

Endometrial cancer is staged based on the International Federation of Gynecology and Obstetrics (FIGO) system, which underwent an updated major revision in 2009.[20,23]

Based on the 2009-revised FIGO staging system, tumors confined to the endometrium, as well as those invading the inner half of the myometrium, are designated as stage IA tumors.[24]

Tumors invading the outer half of the myometrium are designated as stage IB tumors. MR imaging is highly accurate in distinguishing stages IA and IB tumors.[25] With the old staging system, differentiating between stages IA and IB tumors could be challenging in patients with loss of junctional zone definition or in lesions with poor tumor-to-myometrium contrast, both of which

Table 2
Parameters of dynamic contrast-enhanced magnetic resonance imaging for uterus lesion characterization in our institution

TE	TR	FOV	Slice	Space	Matrix	NEX	Direction Frequency	Fat Saturation	Pulse Sequence
Minimum	5675	40	3.0 mm	0.5	128 × 192	16	R-L	Chemical suppression	T1W 3DFSRG

Abbreviations: FOV, field of view; R-L, right to left; TE, echo time; TR, repetition time; T1W, T1-weighted.

are common pitfalls in endometrial cancer staging. The fusion of stage IA and IB tumors into a new stage IA should alleviate this problem.

Stage II tumors are those with cervical stromal invasion. In the new staging system, subsets IIA and IIB no longer exist, and tumors with endocervical glandular invasion are now considered stage I tumors.[25]

Stage III is still composed of 3 subdivisions: IIIA, IIIB, and IIIC. Stage IIIA tumors invade the serosa or adnexa, and stage IIIB tumors invade the vagina or parametrium. Previously, stage IIIC referred to any lymphadenopathy (pelvic or retroperitoneal); in the new FIGO system, however, stage IIIC is divided into stage IIIC1, which is characterized by pelvic lymph node involvement, and stage IIIC2, which is characterized by para-aortic lymph node involvement.[25]

These changes reflect prognostic data that suggest a worse outcome in patients with involvement of para-aortic nodes than in those with involvement of pelvic nodes only.[26]

Stage IV remains unchanged: stage IVA tumors extend into adjacent bladder or bowel, and stage IVB tumors have distant metastases (**Table 4**).

After administration of contrast media, endometrial tumors enhance earlier than normal endometrium, which aids in the detection of small tumors.

Normal myometrium enhances intensely compared with hypointense endometrial tumor. Maximum contrast between hyperintense myometrium and hypointense endometrial tumor occurs 50 to 120 seconds after contrast media administration. Therefore, evaluation of the depth of myometrium invasion should be done at this stage (FIGO stage I).[25,27] Delayed-phase images obtained 3 to 4 minutes after contrast media administration are useful in detecting cervical stromal invasion (FIGO stage II). The presence of an intact enhancing cervical mucosa excludes stromal invasion (**Fig. 10**).[25]

DCE images, when evaluated along with T2-weighted images, have a diagnostic accuracy of up to 98% for assessing myometrium invasion.[25,28,29]

There is some controversy in the literature regarding the added value of DCE-MR imaging for overall FIGO staging, however. Although most published studies have shown an improvement in staging accuracy with DCE-MR imaging, some investigators have found no benefit.[25]

In the authors'opinion, the DCE images have advantages over the T2-weighted images and both should be used to better stage the lesion.

DWI DWI is a functional imaging technique that displays information about water mobility, tissue cellularity, and the integrity of the cell membranes.[29]

On DWI, endometrial cancer manifests as a high-SI mass, hypointense on the corresponding ADC map, in comparison with normal endometrium.[1,30,31]

The combination of conventional MR images and DWI seems particularly useful in assessing the depth of myometrial invasion by endometrial cancer, when there is thinning of the myometrium, or in differentiating cancer from coexisting leiomyomas or adenomyosis (**Fig. 11**).

Table 3
Parameters of dynamic contrast-enhanced magnetic resonance imaging for adnexal lesion characterization in our institution

TE	TR	FOV	Slice	Space	Matrix	NEX	Direction Frequency	Fat Saturation	Pulse Sequence
Minimum	5675	40	3.0 mm	0.5	128 × 192	16	R-L	No	T1W 3DFSRG

Abbreviations: FOV, field of view; R-L, right to left; TE, echo time; TR, repetition time; T1W, T1-weighted.

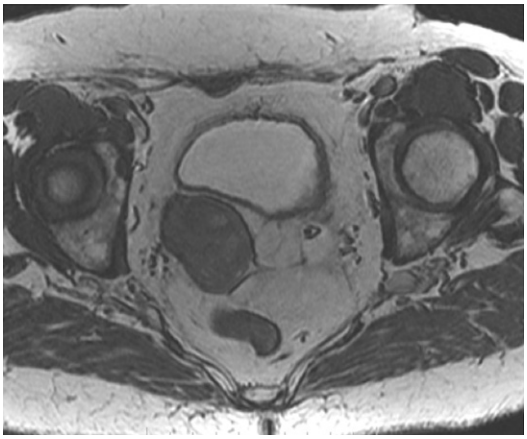

Fig. 9. Adnexal right adenocarcinoma. Three-dimensional FIESTA sequence is acquired with similar parameters.

In one study,[32] all staging errors at contrast-enhanced MR imaging were overcome by incorporating DWI.

Rechichi and colleagues[33] found that ADC values may provide useful and reliable information in differentiating normal endometrium and myometrium from malignant endometrial tissue. In this study, the mean ADC value of endometrial cancer was 0.77 $\pm$ 0.12 10^{-3} mm^2/s (average size of ROIs, 35 pixels; first–third quartiles, 29–39 pixels), which was significantly lower ($P<.0001$) than that of normal endometrium in the control group (1.31 $\pm$ 0.11 10^{-3} mm^2/s; average size of ROIs, 36 pixels; first–third quartiles, 29–40 pixels) and that of normal myometrium (1.52 $\pm$ 0.21 10^{-3} mm^2/s; average size of ROIs, 33 pixels; first–third quartiles, 29–37 pixels). There was no overlap between the 2 former distributions; therefore, it was possible to define a clear cutoff ADC value of 1.05 10^{-3} mm^2/s to distinguish between endometrial cancer and normal endometrial tissue.

Although T2-weighted imaging provides usually reliable contrast for tumor depiction, DWI may be clinically relevant in the following 2 scenarios: (1) isointense tumors, as seen in diffusely infiltrative adenocarcinomas in young women, and (2) early cervical cancer extension for exact delineation of tumor margins, if fertility-preserving surgery is planned.[1]

In a recent prospective study by Rechichi and colleagues,[34] the staging accuracy of diffusion-weighted MR imaging was superior to that of DCE-MR imaging and had a higher level of interobserver agreement.

Beddy and colleagues[29] also found a higher level of interobserver agreement of DWI when compared with DCE-MR imaging.

DWI and DCE-MR imaging are useful adjuncts to standard morphologic imaging and may improve overall staging accuracy of the endometrial carcinoma. Also, DWI can play an important role in patients who cannot accept contrast agent, such as those with renal failure.

Miometrium

Miometrial focal lesions

Leiomyomas are common benign tumors that usually are asymptomatic and may have different imaging appearances. Most leiomiomas tend to contain hyalinized collagen. Therefore, on MR imaging, uterine leiomyomas are well circumscribed, isointense to the muscle on T1-weighted images, and hypointense on T2-weighted images.[35]

These tumors are well circumscribed and surrounded by a pseudocapsule, and some of them present with a thin hyperintense rim of dilated

Table 4
Endometrial cancer International Federation of Gynecology and Obstetrics system, 2009 revision

Endometrial Cancer	Stage A	Stage B	Stage C	
Stage I	Confined to the endometrium <50% of the myometrium	Invading >50% of the myometrium	—	
Stage II	Endocervical glandular invasion			
Stage III	Invades the serosa or adnexa	Invades the vagina or parametrium	C1. pelvic lymph node	C2. Para-aortic lymph node
Stage IV	Invades bladder or bowel	Distant metastases	—	

Dynamic contrast imaging.

Data from Sala E, Wakely S, Senior E, et al. MRI of malignant neoplasms of the uterine corpus and cervix. AJR Am J Roentgenol 2007;188:1577–87; and Creasman W. Revised FIGO staging for carcinoma of the endometrium. Int J Gynaecol Obstet 2009;105(2):109.

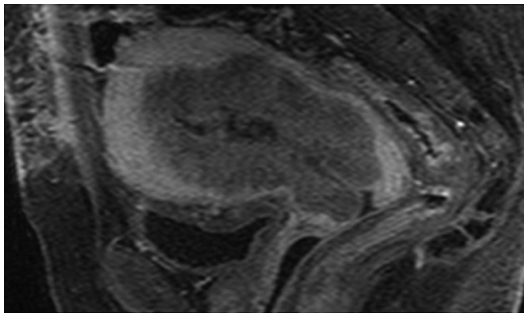

Fig. 10. Endometrial carcinoma with myometrial and cervical invasion. DCE-MR imaging. Three-dimensional T1-weighted fast-spoiled gradient-recalled sagittal section.

lymphatic clefts and dilated veins; edema may be seen on T2-weighted images and helps differentiate leiomyomas from focal adenomyosis.[9]

Degenerated leiomyomas have variable appearances on T1-weighted, T2-weighted, and contrast-enhanced images, such as (1) cellular leiomyomas, composed of compact smooth muscle cells with little or no collagen, can have relatively higher SI on T2-weighted images and marked enhancement on the contrast-enhanced images; (2) cystic degeneration shows high SI areas on T2-weighted images that do not enhance; (3) myxoid degeneration shows very high SI on T2-weighted images and enhances minimally on contrast-enhanced images; and (4) red degeneration exhibits peripheral or diffuse high SI on T1-weighted images and variable SI with or without a low-SI rim on T2-weighted images, and no enhancing areas (**Fig. 12**).

These imaging aspects can affect the aspects of uterine leiomyomas in functional images.

On MR imaging, uterine sarcomas often manifest as a large, infiltrating myometrial mass of intermediate to high SI on T2-weighted images. Differentiation between benign degenerated leiomyoma and malignant tumors may be difficult if based only on SI of nonenhanced and postcontrast MR sequences.

DWI Most leiomyomas tend to contain hyalinized collagen, so their signal is hypointense on T2-weighted images. The DWI appearance of these leiomyomas can be explained by a "T2 blackout effect" (ie, hypointensity on DWI due to hypointensity on T2-weighted images), which causes a decrease in the ADC of ordinary leiomyomas. As a consequence, all of the ordinary leiomyomas have low SI on DWI (**Fig. 13**).

Although MR imaging usually allows specific diagnosis of the much more common benign leiomyomas, degenerated leiomyomas may occasionally be associated with various types of cellular histologic subtypes, which can cause increased signal on T2-weighted images. Cellular leiomyomas can exhibit high SI on DWIs, simulating uterine sarcomas (**Fig. 14**).[36]

Bakir and colleagues[37] suggested that DWI is not useful in the differential diagnosis of degenerated benign and malignant myometrial lesions. Degenerated leiomyomas and leiomyosarcomas displayed varied signal intensities. The ADC value of leiomyosarcomas was lower than those of degenerated leiomyomas with no overlap, but this difference was not statistically significant. Furthermore, the ADC values of ordinary leiomyomas

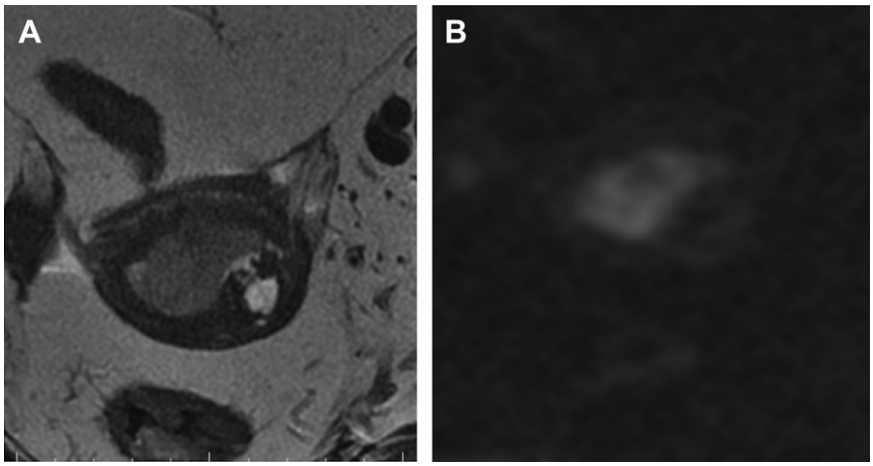

Fig. 11. Endometrial cancer confined to the endometrium and coexisting posterior adenomyosis. (*A*) Coronal oblique T2-weighted image. (*B*) DWI was useful in assessing absence of myometrial invasion.

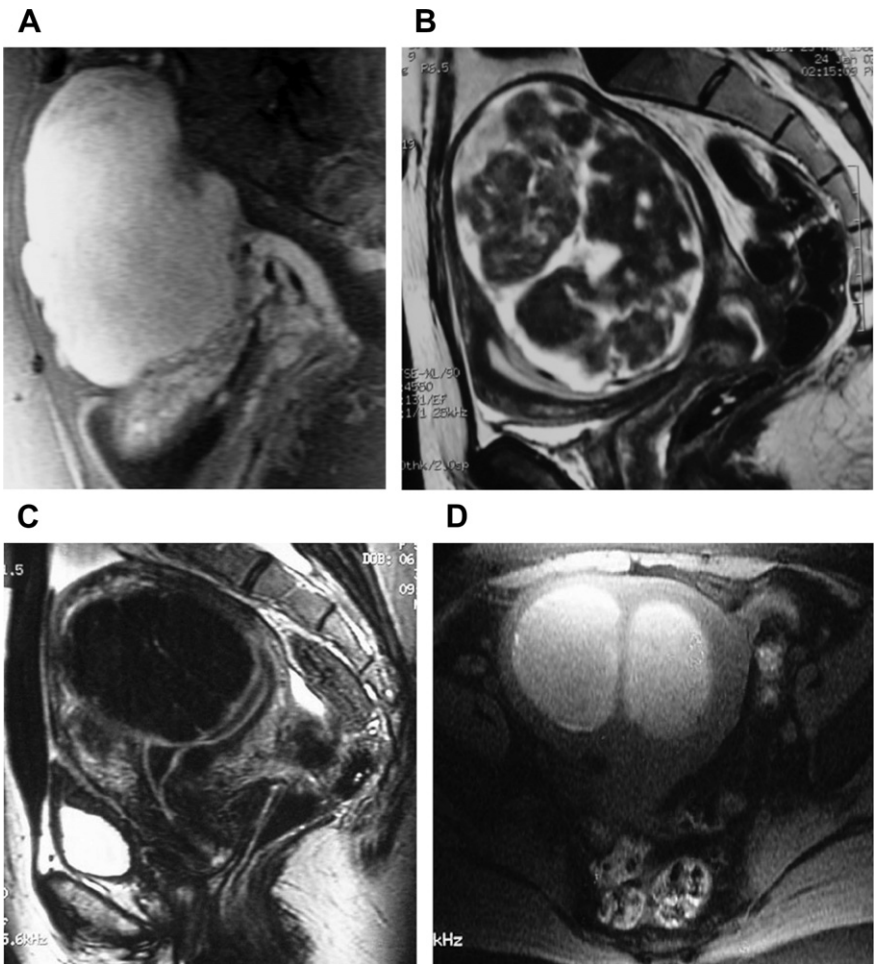

Fig. 12. Leiomyomas. (*A*) Cellular leiomyoma with marked enhancement on contrast-enhanced images. (*B*) Myxoid degeneration with high SI focus on T2-weighted images. (*C*) Hyalinized leiomyoma. Well-circumscribed mass, hypointense on T2-weighted images. (*D*) Red degeneration exhibits diffuse high SI on T1-weighted image.

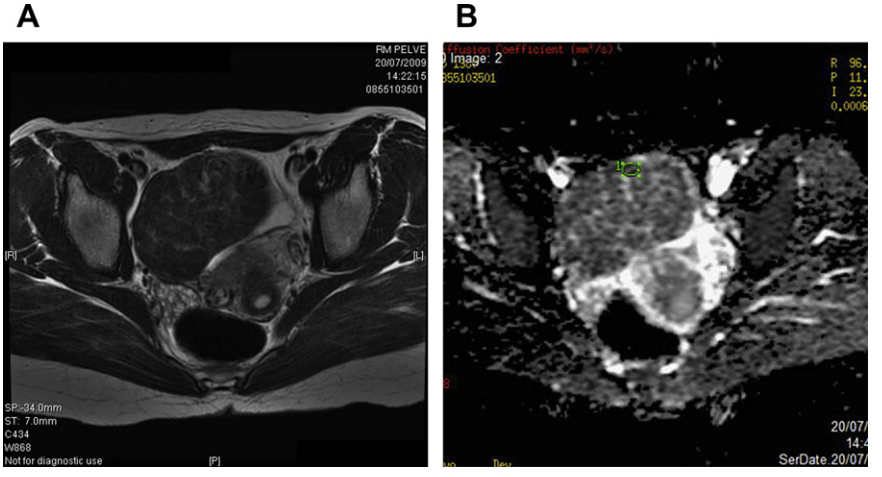

Fig. 13. Hyalinized leiomyoma. (*A*) Hypointense on T2-weighted image. (*B*) Hypointense signal on the ADC map.

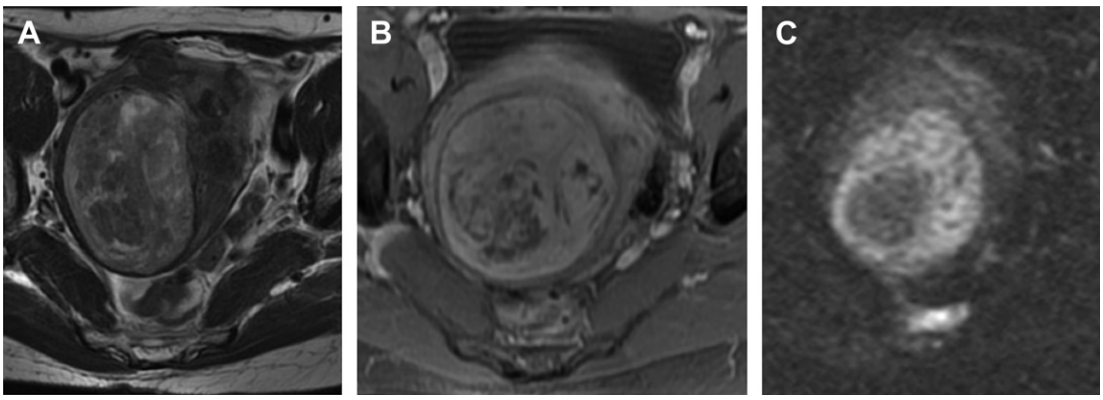

Fig. 14. Cellular leiomyomas. Well-circumscribed mass with higher SI on T2-weighted images, marked enhancement on contrast-enhanced images, and high SI on DWIs. (*A*) T2-weighted image. (*B*) Postcontrast image. (*C*) DWI.

overlapped with those of both degenerated leiomyomas and leiomyosarcomas.[37]

However, Tamai and colleagues[36] and Takeuchi and colleagues[38] reported that DWI could be useful in differentiating hyperintensity on T2-weighted images of leiomyomas from malignant lesions. All malignant tumors showed high SI on DWI with low ADC, which was significantly lower ($P<.01$) than that in benign leiomyomas. The ADC in cellular leiomyoma (1.18) was significantly lower than that in degenerated leiomyoma (1.60) and higher than that in malignant tumors. They concluded that the ADC measurement might be helpful in distinguishing benign from malignant tumors.

Recent studies have demonstrated the use of DWI to obtain "functional parameters" in both untreated and treated uterine lesions. MR imaging–guided focused ultrasound-treated leiomyoma demonstrated restricted diffusion. The heat obtained from this procedure changes the motion of water and disrupts the bound and unbound proteins within the tissue. Release of these proteins maybe the reason for the decreased water movement after this treatment. The ADC value exhibited a high similarity index and good correlation between the volumes of treated tissue. DWI could be useful as an adjunct for assessing response to treatment in uterine fibroids by MR imaging–guided focused ultrasound.[39]

Adenomyosis Adenomyosis is a common nonneoplastic gynecologic disease characterized by the presence of ectopic endometrium within the myometrium.

Adenomyosis is detected on T2-weighted images as thickening of the junctional zone to 12 mm or more, often associated with punctuate foci of high SI. Although the thickness of the junctional zone has been reported to vary from 2 to 8 mm, the use of a lower threshold may result in false-positive diagnosis of adenomyosis because of sustained myometrial contractions, uterine peristalsis, and diffuse physiologic thickening of the junctional zone during menstruation.[9]

Typical adenomyosis appears as an ill-demarcated low-SI area on T2-weighted images owing to abundant smooth muscle proliferation. Because adenomyotic endometrium looks like the basalis endometrium, which seldom responds to hormonal stimuli, cyclic changes, including degeneration, bleeding, and regeneration, are less common in adenomyosis than in endometriosis. On T2-weighted MR images, ectopic endometrium appears as small high-SI areas similar to normal endometrium. Small cysts may also appear as high-SI spots on T2-weighted images. Sometimes, hemorrhagic foci appear as high-SI foci on T1-weighted images owing to the T1-shortening effects of methemoglobin.[40,41]

Small hemorrhagic foci (hemosiderin deposition), which are barely detectable on T2-weighted images, can be demonstrated as signal voids on susceptibility-weighted images.[41]

Susceptibility-weighted MRI is a relatively new MR technique that maximizes sensitivity to susceptibility effects and has exquisite sensitivity to blood products, such as hemosiderin and deoxyhemoglobin, and can depict discrete adenomyotic changes in the myometrium (**Fig. 15**).[41,42]

Cervix

Cervical cancer

Uterine cervical cancer is one of the most common malignancies seen by gynecologic radiologists.[43] In spite of advances in treatment enabling women to live longer, there remains a substantial associated mortality.[43]

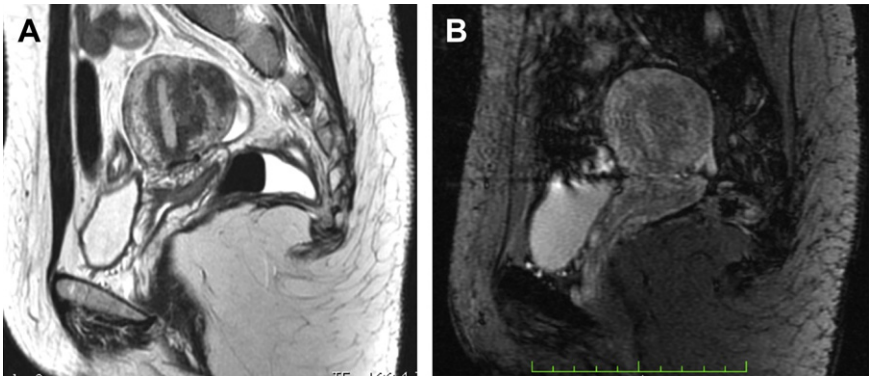

Fig. 15. Adenomyosis. (*A*) Sagittal T2-weighted image shows posterior corporal thickened junctional zone with a hyperintense foci of heterotopic endometrial tissue. (*B*) Sagittal susceptibility-weighted MRI depicted discrete hypointense foci within the adenomyotic changes in the myometrium.

Most cervical squamous cell carcinomas grow at the squamocolumnar junction (SCJ). In younger women, the SCJ is located outside the external uterine os, and the tumor tends to grow outward (exophytic growth pattern). In contrast, in older patients, the SCJ is located within the cervical canal. In these patients, cervical cancer tends to grow inward along the cervical canal (endophytic growth pattern).[43]

MR imaging can provide highly accurate information on the exact extent of cervical tumors because of its fine contrast resolution. Cervical cancers appear as hyperintense masses on T2-weighted images regardless of its histopathologic type.[43]

DWI The applications of DWI in the assessment of cervical cancer are differentiating normal from cancerous tissues and evaluating response to chemo-radiotherapy. Cervical cancer shows restricted diffusion related to an increase in cellular density, tissue disorganization, intact cellular membranes, and increased extracellular space tortuosity, features that collectively restrict the diffusibility of water molecules (**Fig. 16**).

The ADC value of cervical cancer lesions has been reported to be lower than that of normal cervical tissues, and ADC increases after chemotherapy or irradiation.[44,45]

McVeigh and colleagues[46] found that the median ADC of cervical cancers was significantly lower than the median ADC of normal cervix stroma, with very little overlap between the 2 cases. The average mean ADC for cancerous tissue was 1.09 $\pm$ 0.20 $\times$ 10^{-3} mm^2/s, whereas that of the control cervical tissue was 2.09 $\pm$ 0.46 $\times$ 10^{-3} mm^2/s (see **Fig. 16**).

Furthermore, Somoye and colleagues[47] investigated whether DWI performed early in the treatment of locally advanced cervical cancer could

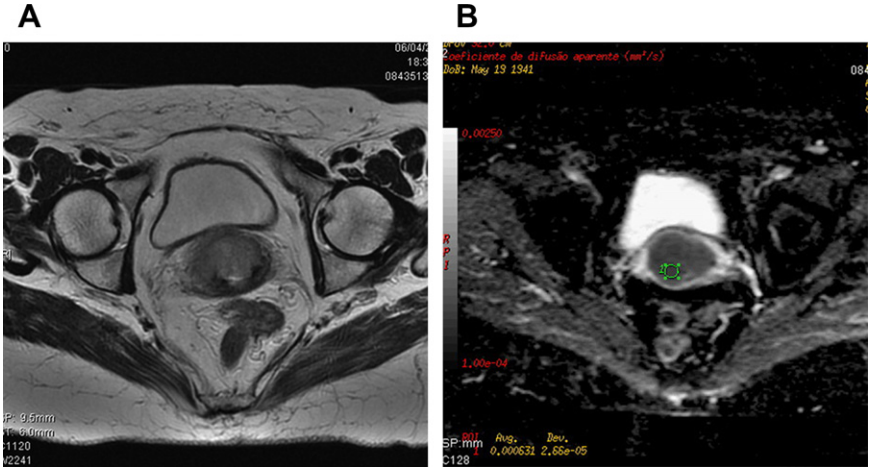

Fig. 16. Cervical carcinoma. Cervical isointense mass presenting with hypointense signal on the ADC map.

predict survival. Their study revealed an ADC difference between pretherapy ADC and ADC values at 2 weeks after treatment, indicative of tumor response; however, there was no evidence that pretreatment or post-therapy ADC variables and baseline tumor volumes were related to response.

DCE-MR imaging Although DCE-MR imaging does not significantly improve staging accuracy compared with standard T2-weighted images, it may be additionally applied for detection of early-stage cervical cancer. Moreover, some investigators have suggested that the functional assessment of the microcirculation using DCE-MR imaging would predict therapy outcome in cervical cancer, in addition to traditional factors, such as stage, extent of disease, histologic type, lymphatic spread, and vascular invasion.[44]

In a pre–radiation therapy study, a favorable outcome was demonstrated in patients with strong tumor enhancement, suggesting good tumor oxygenation. Tumors with baseline higher permeability (Ktrans) tend to show a better response to radiotherapy. After radiotherapy, tumor enhancement has been delayed compared with that before therapy.[48]

Yamashita and colleagues[49] also found that the pattern of enhancement or increased permeability in the region of the tumor correlated with the incidence of durability or local recurrence. Tumors with a homogeneous enhancement pattern showed significantly better treatment results than those with a peripheral enhancement pattern or those with predominantly poor enhancement. Tumors with increased permeability also had a higher incidence of good response to treatment.

Manelli and colleagues[50] found an inverse correlation between the percentages of nonenhancing tumor tissue evaluated using pretreatment DCE-MR imaging subtracted images and percentages of tumor regression after chemoradiotherapy in patients with advanced cervical cancer. The presence of hypoxic cells is one of the most important factors affecting tumor resistance to radiotherapy and overall prognosis in patients with advanced cervical cancer. Minimally necrotic tumors show a more homogeneous enhancement, and they have a better prognosis. These tumors are more likely to be well oxygenated and therefore more sensitive to radiation and have a better perfusion, which will also result in a higher concentration of chemotherapeutic agent within the tumor. The nonenhancing tumor areas can be necrotic, can have less biologic activity than the tumor cells, and are likely hypoxic and more resistant to therapy. Patients presenting with these tumors have a worse prognosis.[13,49]

ADNEXA

Advances in Adnexal Imaging

MR evaluation of adnexal lesions should be based on 2 features: morphology and SI. Reported morphologic signs of malignancy include bilaterality, diameter larger than 4 cm, predominantly solid mass, and cystic tumor with vegetation or intramural nodule, as well as secondary malignant features, such as ascites, peritoneal involvement, and enlarged lymph nodes (**Box 1**).[51]

The other criteria are related to the T1 and T2 contrast. The low signal of solid components on T2-weighted imaging is suggestive of benign fibrous tissue (observed in cystadenofibroma, ovarian fibroma, and Brenner tumor), with an overall accuracy of about 68% according to Sohaib and colleagues.[52] High SI on T1-weighted images is highly suggestive of benign disease, observed in lesions presenting with fat (such as benign teratoma) or blood products (endometrioma) (**Fig. 17**).[53]

For hyperintense lesions, there is no need for further characterization; however, the other reported criteria are not specific predictors of malignancy, because an overlap between benign and malignant tumors may be seen, especially in the diameter and bilaterality.

Umemoto and colleagues[53,54] reported that a solid component in an ovarian mass was the most statistically significant predictor of malignancy on MR imaging, but the accuracy of this feature is less than 50%.

Functional sequences are promising emerging techniques for better characterization of ovarian masses, based on diffusion and perfusion characteristics. Another useful technique is the susceptibility-weighted sequence, which maximizes sensitivity to susceptibility effects related to the presence of blood products, allowing

Box 1
Morphologic signs of malignancy on MR imaging

- Solid and cystic areas within a lesion
- Necrosis within a solid lesion
- Irregular multiple thickened septum or irregular thickened wall
- Papillary projections
- Large size (>6 cm)
- Bilateral lesions
- Ascites, peritoneal disease, or lymphadenopathy

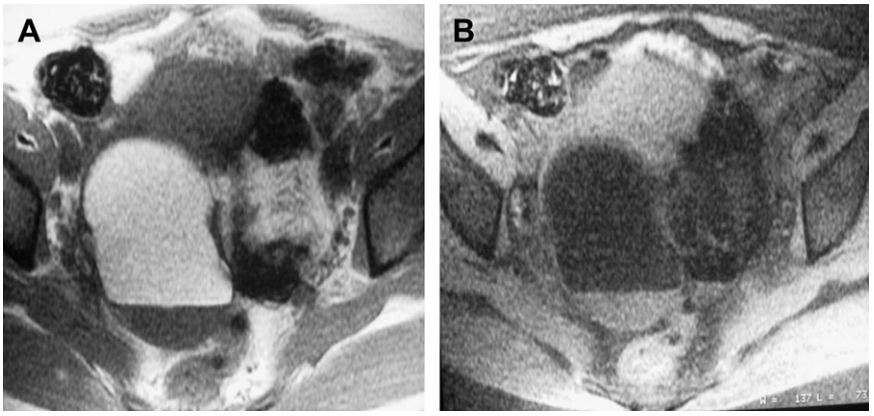

Fig. 17. Right adnexal teratoma. Lesion shows high SI on T1-weighted image, and low SI on T1-weighted image with fat suppression. (*A*) T1-weighted image. (*B*) T1-weighted image with fat suppression.

distinction between an old endometrioma and a fibrotic solid lesion.[40]

Susceptibility-weighted MRI

Endometrioma

Endometriomas are the most common manifestation of pelvic endometriosis. They are cysts with hematic content of different ages, composed of endometrial glands and stroma, which promote cyclic bleeding, resulting in hemosiderin deposition.[54]

Multiple hyperintense cysts on T1-weighted images and a hyperintense cyst on T1-weighted images that also has hypointense signal on T2-weighted images (shading) are considered definite MR imaging signs of endometrioma and have 90% sensitivity, 98% specificity, and 96% accuracy for the diagnosis.[40,42,55]

Some endometriomas, however, are filled with watery fluid on gross cut sections and may not exhibit typical MR imaging findings.[42] In such cases, visualization of hemosiderin deposition in the cyst wall may be helpful.[40]

Susceptibility-weighted MR imaging is a relatively new MR imaging technique that maximizes sensitivity to susceptibility effects and has exquisite sensitivity to blood products, such as hemosiderin and deoxyhemoglobin.[40,42]

The magnetic susceptibility effects generated by local inhomogeneity of the magnetic field caused by hemosiderin or deoxyhemoglobin is visualized as signal voids.[40]

Takeuchi and colleagues[40] found signal voids following magnetic susceptibility in 39 (92.9%) of 42 endometriomas, demonstrating the usefulness of this sequence.

It is important to note that the content of nonendometrial hematic cysts had no signal voids along the cyst walls on susceptibility-weighted images, which was attributed to the fact that these cysts do not repeatedly bleed. Thus, the finding of a thick capsule containing a cluster of hemosiderin-laden macrophages is specific for the diagnosis of endometrioma and susceptibility-weighted imaging is especially sensitive to this finding (**Fig. 18**).[40]

DWI

Tubo-ovarian abscess

Tubo-ovarian abscess (TOA) is a late complication of pelvic inflammatory disease (PID) and involves a frank abscess or an inflammatory mass resulting from breakdown of the normal structure of fallopian tubes and ovaries by inflammation. The clinical features of TOA and uncomplicated PID are similar, and differentiation is usually achieved with imaging examination.[56]

DWI is a well-established method for studying infectious diseases, especially intracranially, as well as in the breasts and abdomen.[57]

TOAs may produce complex masses with wall thickening and pseudosolid areas, thereby mimicking malignancy. The pseudosolid areas can demonstrate different SI on T1-weighted and T2-weighted images, and marked enhancement, related to high inflammatory cellularity, a matrix of proteins, cellular debris, and bacteria in high-viscosity purulent fluids, as well as large molecules playing a key role in restricting the diffusion of protons in pus. Moreover, the clinical features are not specific, and can mimic malignancy.[58]

Li and colleagues[57] found an increase of 22.5% in the diagnostic confidence of conventional MR imaging in the diagnosis of TOA using DWI. The improvement in diagnostic confidence was related to the addition of DWI to conventional MR imaging, which can differentiate pseudosolid

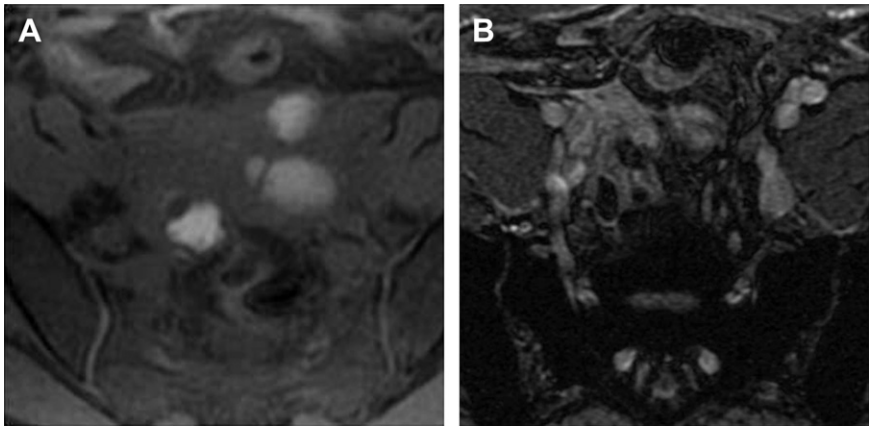

Fig. 18. Endometrioma. Hyperintense cyst on axial T1-weighted image with fat suppression and signal voids along the cyst walls on the susceptibility-weighted image. (*A*) T1-weighted image. (*B*) Susceptibility-weighted image.

(pus) from other conditions, such as the mucinous components of adnexal tumor, based on signal characteristics.[57]

Li and colleagues[57] considered that the best criteria for predicting an abscess, was the finding of a mass presenting with high or intermediate SI on T2-weighted images, no enhancement, and high SI on DWI, along with low ADC values. In this publication, DWI could also characterize and differentiate pyosalpinx from hydrosalpinx. Both of those demonstrated dilated, fluid-filled tubal structures, with variable SI on T1-weighted and T2-weighted images, but only pyosalpinx demonstrated low SI on the ADC map, related to the viscosity and high protein concentrations of the fluid contained in the pus in a pyosalpinx.[57]

Takeshita and colleagues[58] suggested that TOA presented with restricted diffusion similar to brain abscess. Thus, DWI can be an alternative for the diagnosis of TOA when the contrast study cannot be performed. The SI on the ADC map, along with the ADC measurements, may allow the correct diagnosis of TOA (**Fig. 19**).

Adnexial torsion

Ovarian torsion is the twisting of an ovary on its ligamentous supports and can result in a compromised blood supply. Adnexial torsion is a loose term that may refer to torsion of the ovary, the fallopian tube, or both. Concomitant ovarian and tubal torsion has been shown to occur in up to 67% of cases of adnexal torsion (**Fig. 20**).[59,60]

Large, heavy cysts and cystic neoplasms, such as benign mature cystic teratomas, hemorrhagic cysts, and cystadenomas, commonly predispose the ovary to swing on its vascular pedicle.[61] The

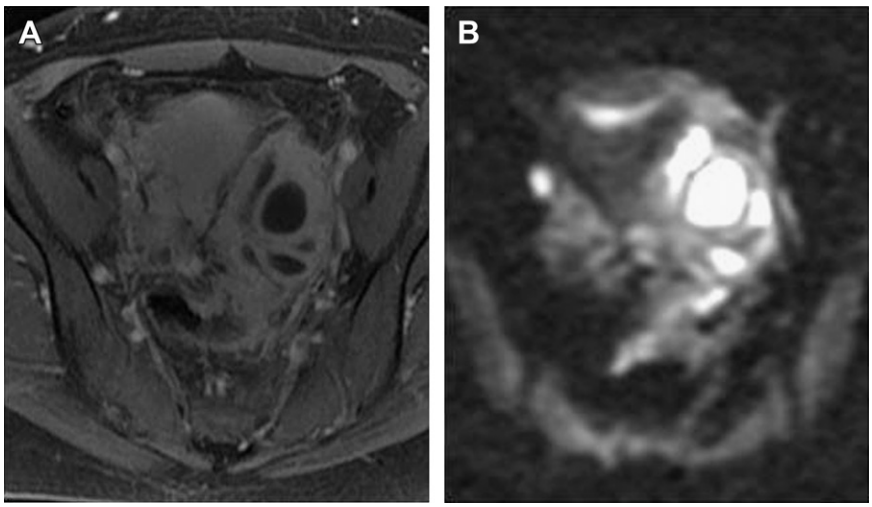

Fig. 19. TOA. Mass with heterogeneous enhancement and high SI on DWI. (*A*) Axial postcontrast image. (*B*) DWI.

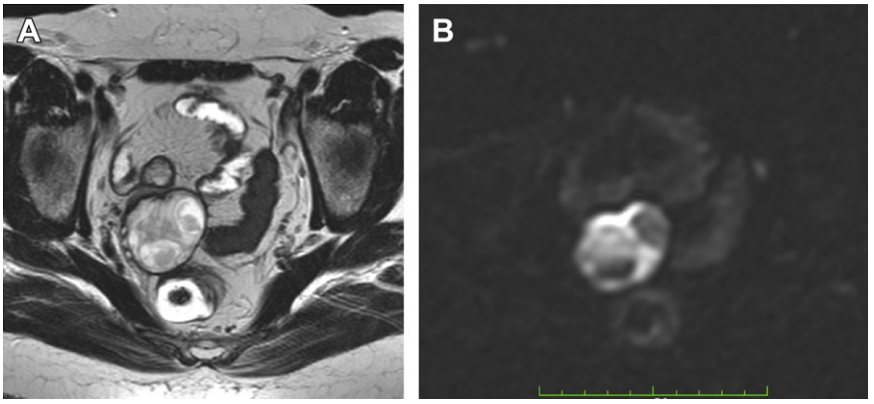

Fig. 20. Ovary edema. Axial T2-weighted image shows enlarged edematous right ovary with peripheral follicles. DWI shows restricted diffusion. (*A*) Axial T2-weighted image. (*B*) DWI.

large cystic ovaries seen in ovarian hyperstimulation syndrome are another predisposing factor for torsion. Conversely, it is rare to see ovarian torsion from cysts smaller than 5 cm.[62]

The SI of the tubal fluid is related to the presence of hemorrhage from fallopian tubal torsion and hematosalpinx and may have a similar appearance on T1-weighted and T2-weighted sequence as well as on the DWI, generally presenting with high SI on conventional images, with restricted diffusion and low ADC values.

DW imaging alone is not useful for differentiating tubal torsion and hematosalpinx from TOA and ovarian abscesses.[57]

Adnexial neoplasms

Ovarian cancer accounts for 3.7% of all cases of cancer in women.[63] Primary ovarian neoplasms are broadly categorized as surface epithelial, germ cell, or sex cord–stromal tumors and may be benign, borderline, or malignant.[64]

Surface epithelial tumors account for most ovarian neoplasms; the most common types being serous, mucinous, and endometrioid. Less common types include clear cell, transitional cell (Brenner and non-Brenner variants), and mixed epithelial tumors.[65]

MR imaging plays a crucial role in characterizing adnexal masses that are indeterminate at ultrasound and determining the origins of pelvic masses. Both MR imaging and ultrasonography have high sensitivity (97% and 100%, respectively) for depicting malignant adnexal masses. However, MR imaging has much higher specificity (84%) and accuracy (89%) for depicting malignant characteristics when compared with Doppler ultrasound (40% specificity and 64% accuracy). Therefore, an adnexal mass that appears suspicious at ultrasound may be correctly diagnosed as a benign lesion at MR imaging, preventing inappropriate radical surgery.[66]

MR imaging characteristics that are indicative of benignity include high SI on T1-weighted images (indicative of fat or blood), loss of SI on fat-suppressed images (indicative of fat), high SI on T1-weighted fat-suppressed images (indicative of blood), and low SI on T2-weighted images (indicative of fibrous tissue or hemosiderin). In particular, solid adnexal tissue that demonstrates low SI on T2-weighted images has been shown to be highly indicative of a benign or noninvasive lesion.[11,57]

On MR imaging performed with conventional protocols, morphologic features that are indicative of a malignant adnexal mass include the presence of both solid and cystic areas within a lesion; necrosis within a solid lesion; papillary projections from the wall or septum in a cystic lesion; an irregular septum or wall; multiple thickened (>3 mm)

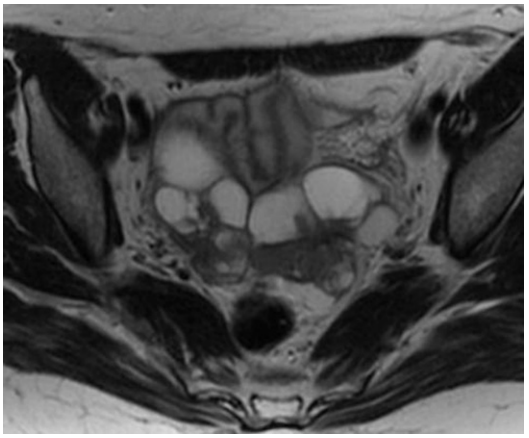

Fig. 21. Bilateral cystic adenocarcinoma showing morphologic features indicative of a malignant adnexal mass. Solid cystic mass, with irregular and thickened septations. Axial T2-weighted image.

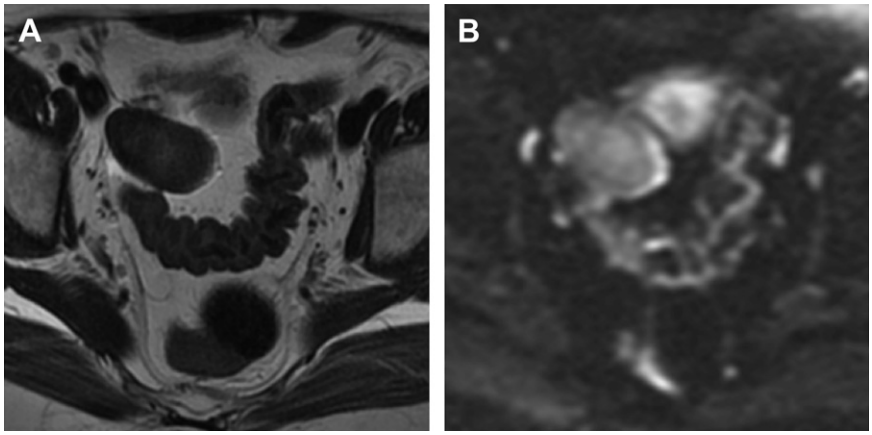

Fig. 22. Fibrotecoma. Solid adnexial lesion showing low SI on the T2-weighted and DW images. (*A*) Axial T2-weighted image. (*B*) DWI.

septations; a large size (>6 cm); bilateral lesions; and ascites, peritoneal disease, or lymphadenopathy (Fig. 21).[52,56]

Functional sequences are promising emerging techniques for better characterization of ovarian tumors. According to Takeuchi and colleagues, the mean ADC values of benign and malignant ovarian tumors differed significantly. Using a cutoff value of 1.15×10^{-3} mm^2/s for the ADC, differentiation of benign from malignant/borderline lesions could be done with 74% sensitivity, 80% specificity 94% positive predictive value (PPV) and 44% negative predictive value (NPV).

A cutoff ADC value of 1.0×10^{-3} mm^2/s had a sensitivity of 46%, specificity of 100%, PPV of 100%, and NPV of 32%.[67]

Thomassin-Naggara and colleagues[68] evaluated 77 solid adnexial lesions, and demonstrated that all solid lesions that presented with low SI on DWI acquired at a b value of 1000 s/mm^2 were benign (Fig. 22)[56]; however, there were some overlaps between the mean ADC values of the malignant and benign ovarian lesions. Thomassin-Naggara and colleagues[68] considered that their results may reflect the increased mean ADC values in some malignant lesions owing to the existence of small necrotic or cystic areas in solid tumoral components, or fluid collection intervening papillary projections, and the decreased mean ADC values in some benign lesions owing to relative hypercellularity in functioning ovarian tumors, such as thecomas, or restriction of the water diffusion by dense stromal proliferation in fibroma without edematous changes (Fig. 23).[69]

Katayama and colleagues[69] reported that ADC values may provide limited information in the

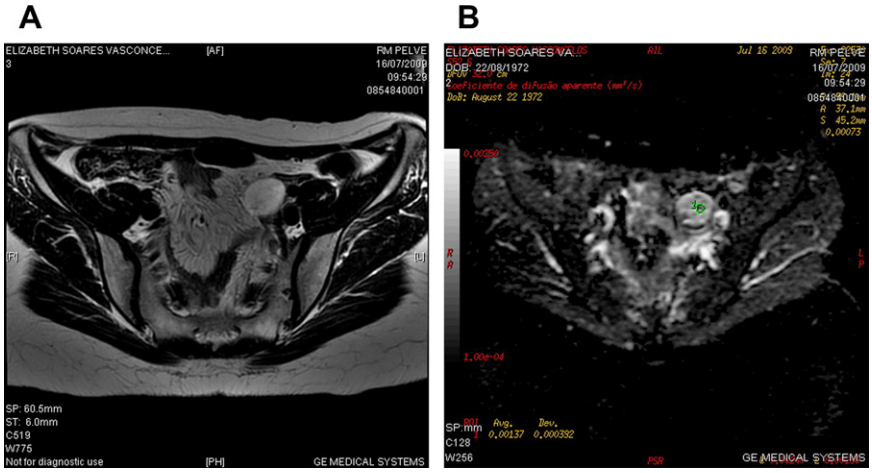

Fig. 23. Limitation of diffusion in the evaluation of cystic ovary lesions. Left ovary malignant lesion showing increased ADC owing to cystic areas within the solid tumoral component.

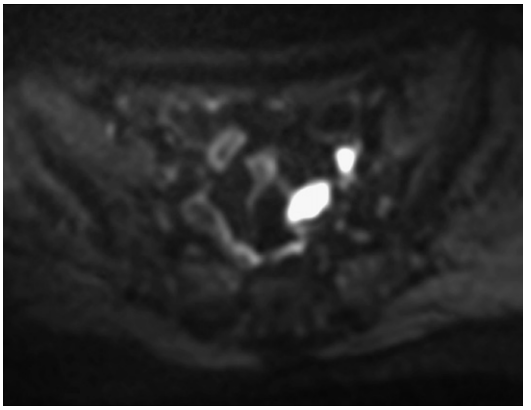

Fig. 24. Left peritoneal implants. High SI on DWI related to restricted diffusion.

differential diagnosis of cystic ovarian tumor, but most of them agree that most solid components of malignant ovarian tumors demonstrated high SI on DWI.[70,71]

When T2-weighted images and DWIs are combined, the most useful findings for predicting malignancy in adnexal masses include the presence of papillary projections (positive likelihood ratio [PLR] = 4.5), high SI on DWIs at b value of 1000 s/mm^2 within the solid component (PLR = 3.1), intermediate SI on T2-weighted images of the solid component (PLR = 2.2), ascites and peritoneal implants (PLR = 2), and a solid portion (PLR = 1.8).[1]

In contrast, the absence of high b value (1000 mm^2/s) signal was highly predictive of benignity (PLR = 10.1). A tumor displaying both low T2 and low b1000 signal was never malignant in this study. The addition of DWI increased the diagnostic confidence in 15% (see **Fig. 22**).[1,52,56]

A few studies have investigated the value of DWI in the assessment of peritoneal spread in gynecologic cancers. Compared with CT and conventional MR imaging, qualitative DWI has been shown to improve staging accuracy by enhancing

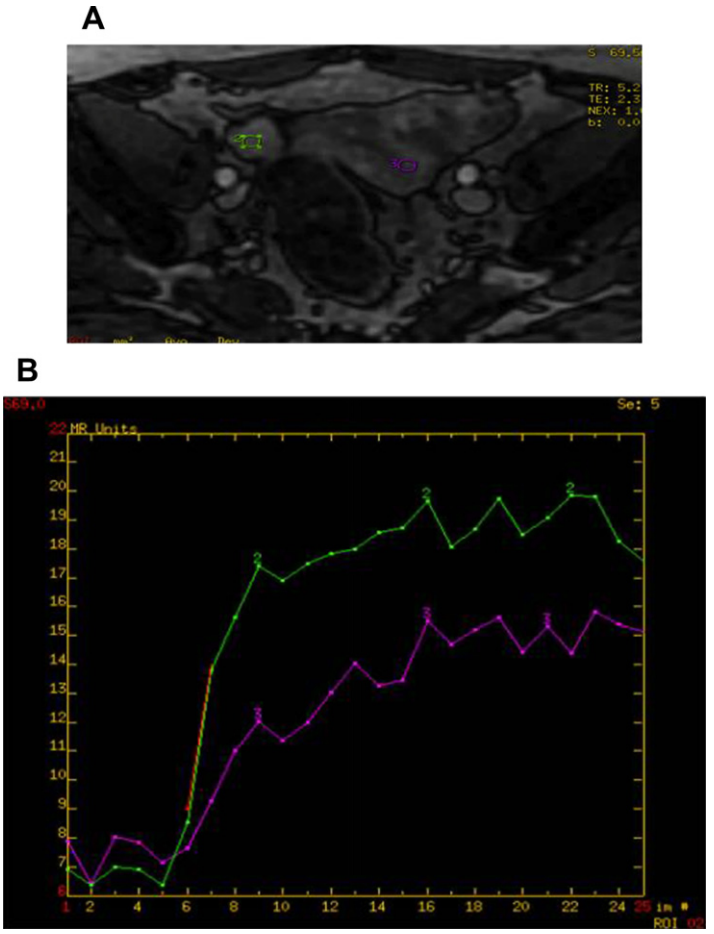

Fig. 25. Sertoli-Leydig tumor. Dynamic contrast imaging shows type III curve. (*A*) DCE-MR imaging. (*B*) Dynamic curve.

the detectability of peritoneal implants and also the detection of small peritoneal implants at sites difficult to assess with routine imaging. An early study reported that fusion of DWI with T2-weighted imaging yielded excellent sensitivity (90%) and specificity (95.5%) for assessing peritoneal spread in ovarian cancer.[1,70]

The highest incremental value of DWI was for metastases in the mesentery and for small bowel and colonic serosal surface implants (**Fig. 24**).[11]

Kyriazi and colleagues[72] demonstrated that, in patients with peritoneal ovarian cancer, DWI was potentially useful for monitoring treatment efficacy. Changes on ADC values correlated with and often preceded size and tumor-marker evidence of response, with a predictive value in assessing chemotherapy response. Response was associated with an early and sustained increase of ADCs and lack of response with stability of all histogram parameters. This is supported by the established inverse correlation between ADC and cell density.[72]

DCE-MR imaging has been used for the characterization of ovarian tumors, and it has been proven useful for distinguishing malignant from

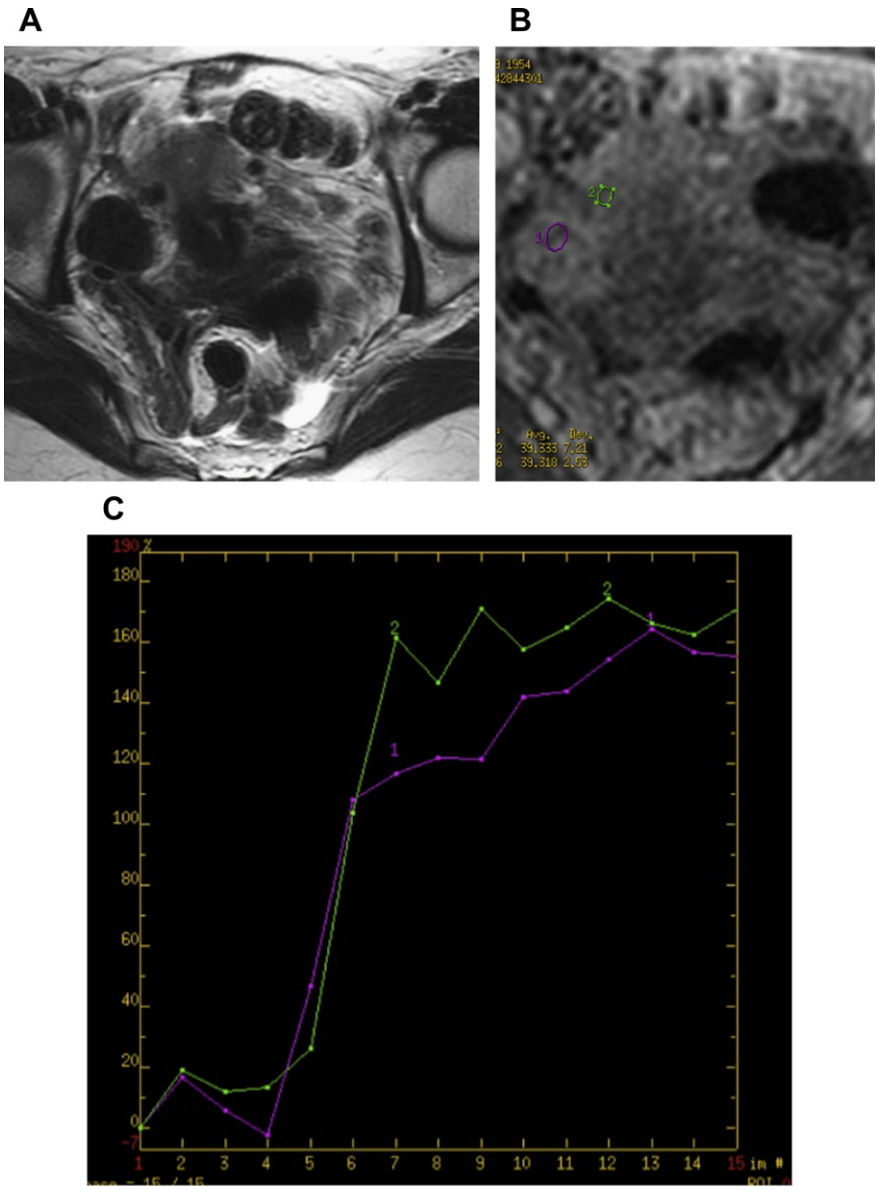

Fig. 26. Ligament right leiomyoma. DCE-MR imaging shows stronger enhancement in the leiomyoma compared with myometrium, with type III curve. (*A*) Axial T2-weighted image. (*B*) DCE-MR imaging. (*C*) Dynamic curve.

benign tumors, enabling noninvasive in vivo assessment of angiogenesis.[68]

Several studies have suggested that contrast-enhanced MR sequences are superior to noncontrast MR imaging for ovarian tumor characterization.[52,68,73] The overall accuracy of this sequence for distinguishing benign from malignant ovarian lesions reaches 90% in some series.[68,73]

Sohaib and colleagues[52] confirmed that malignant tumors exhibited stronger early enhancement (<60 seconds) than benign tumors.

Bernardin and colleagues[10] evaluated 70 complex adnexal masses (solid or mixed solid and cystic) on conventional MR images and DCE images. The parameters used were the tissue SI on unenhanced T1-weighted images (SI0); SI at maximum absolute contrast enhancement (SImax); maximum relative SI (SIrel); and wash-in rate (WIR), the difference between SI0 and SImax divided by time (in seconds). At DCE-MR imaging with semiquantitative analysis, the solid enhancing portion of malignant (borderline or invasive) tumors had significantly higher SImax, SIrel, and WIR values than did benign masses. The WIR proved to be the most significant predictive parameter, with a mean WIR of 11.8 L/s for malignant (borderline or invasive) tumors compared with 6.6 L/s for benign masses ($P<.0001$).

Thomassin-Naggara and colleagues[11] evaluated ovarian tumors with a high temporal resolution DCE-MR imaging technique that allows derivation of accurate time-intensity curves and other early enhancement parameters with an MR imaging workstation and additional computer software. They defined 3 patterns of enhancement of ovarian epithelial tumors, using myometrial enhancement as the internal reference, which correlated with histopathologic findings. This classification of the time-intensity curves of tumor enhancement includes types 1, 2, and 3 curves. Type 1 is a curve showing a gradual increase in the signal of solid tissue, without a well-defined shoulder. Type 2 is a curve with moderate initial rise in the signal of solid tissue relative to that of myometrium, followed by a plateau. Type 3 is a curve with intense initial rise in the signal of solid tissue steeper than that of myometrium. Thomassin-Naggara and colleagues[11] demonstrated that only invasive tumors displayed time intensity curve type 3 (specificity 100%). Enhancement curve types 1 and 2 corresponded to benign and borderline ovarian tumors, respectively. In addition, semiquantitative parameters, like enhancement amplitude, maximal slope, and initial area under the curve within the first 60 seconds ratios were significantly higher for invasive lesions than they were for benign and borderline masses (**Fig. 25**).[11]

Box 2
Adnexial lesions: functional features of malignancy

High SI on DWIs (low on ADC map) in the solid component of a solid/cystic lesion or in the papillary projection

Stronger early enhancement

Type 3 curve on DCE-MR imaging (intense initial rise in the signal of solid tissue, steeper than that of myometrium)

Peritoneal nodes with high signal on DWI and low signal on ADC map

The mechanisms explaining the different enhancement curves are dependent on tissue-specific factors, such as the number and maturity of microvessels, interstitial space, and the interstitial pressure. Malignant tumors demonstrate poorly formed and highly permeable fragile neoangiogenic vessels, explaining a type 3 curve, with intense initial rise in the signal of solid tissue.[74]

Thomassin-Naggara and colleagues[56] identified a correlation between semiquantitative parameters and vascular endothelial growth factor receptor 2 (VEGFR-2) expression. Enhancement amplitude correlated with VEGFR-2 expression on endothelial and epithelial cells, and maximal slope was associated with low smooth muscle actin expression and high VEGFR-2 expression on endothelial and epithelial cells.

DCE-MR imaging has also proved to be useful for distinguishing solid pelvic masses, especially ovarian fibromas and uterine leiomyomas. With normal myometrium used as the reference, enhancement of ovarian fibromas was weaker and slower than that of uterine leiomyomas (**Fig. 26**).[75]

Limitations of this technique include partial coverage of the adnexal mass, the need for the uterus to be present, the requirement that the solid portion of the tumor be at the same level as the myometrium to allow comparisons, and potential variations in myometrial perfusion.[65,76]

Despite their high specificity for depicting invasive lesions, DCE-MR technique is also prone to pitfalls. False-negative results may occur with poorly vascularized malignant tumors, and false-positive enhancement characteristics may be seen in benign lesions with a high blood supply, such as TOA, which may appear complex and indeterminate with all imaging modalities (**Box 2**).[65,76]

SUMMARY

Conventional MR imaging has been widely accepted as a powerful imaging modality for the

evaluation of the pelvis because of its intrinsic superior soft tissue contrast. Functional study with perfusion and diffusion allows the evaluation of microvascular characteristics and cellularity of the lesions. These sequences improve the differentiation of benign from malignant lesions. Moreover, the functional study allows the characterization of lesions, both benign and malignant, thus increasing the specificity of resonance imaging.

REFERENCES

1. Thoeny HC. Genitourinary applications of diffusion-weighted MR imaging in the pelvis. Radiology 2012;263(2):326–42.
2. Hussain SM. MR Imaging of the female pelvis at 3T. Magn Reson Imaging Clin N Am 2007;14:537–44.
3. Thomassin-Nagara I. Characterization of complex adnexal masses: value of adding perfusion- and diffusion-weighted MR imaging to conventional MR imaging. Radiology 2011;258(3):793–803.
4. Le Bihan D, Breton E, Lallemand D, et al. Separation of diffusion and perfusion in intravoxel incoherent motion MR imaging. Radiology 1988;168(2):497–505.
5. Thoeny HC, De Keyzer F, Boesch C, et al. Diffusion-weighted imaging of the parotid gland: influence of the choice of b-values on the apparent diffusion coefficient value. J Magn Reson Imaging 2004; 20(5):786–90.
6. Qayyum A. Diffusion-weighted imaging in the abdomen and pelvis: concepts and applications. Radiographics 2009;29:1797–810.
7. Padhani AR, Harvey CJ, Cosgrove DO. Angiogenesis imaging in the management of prostate cancer. Nat Clin Pract Urol 2005;2:596–607.
8. Alonzi R, Padhani A, Allen C. Dynamic contrast enhanced MRI in prostate cancer. Eur J Radiol 2007;63:335–50.
9. Yankeelov TE, Gore JC. Dynamic contrast enhanced magnetic resonance imaging in oncology: theory, data acquisition, analysis, and examples. Curr Med Imaging Rev 2009;3(2):91–107.
10. Bernardin L. Effectiveness of semi-quantitative multiphase dynamic contrast-enhanced MRI as a predictor of malignancy in complex adnexal masses: radiological and pathological correlation. Eur Radiol 2012;22(4):880–90.
11. Thomassin-Naggara I. Dynamic contrast-enhanced magnetic resonance imaging: a useful tool for characterizing ovarian epithelial tumors. J Magn Reson Imaging 2008;28(1):111–20.
12. Tofts PS, Brix G, Buckley DL, et al. Estimating kinetic parameters from dynamic contrast-enhanced T(1) weighted MRI of a diffusable tracer: standardized quantities and symbols. J Magn Reson Imaging 1999;10:223–32.
13. Manelli L. Evaluation of nonenhancing tumor fraction assessed by dynamic contrast-enhanced MRI subtraction as a predictor of decrease in tumor volume in response to chemoradiotherapy in advanced cervical cancer. AJR Am J Roentgenol 2010;195(2):524–7.
14. Brown MA. MRI of benign uterine disease. Magn Reson Imaging Clin N Am 2007;14:439–53.
15. Lee JK, Gersell DJ, Balfe DM, et al. The uterus: in vitro MR-anatomic correlation of normal and abnormal specimens. Radiology 1985;157:175–89.
16. Gull B, Karlsson B, Milsom I, et al. Transvaginal sonography of the endometrium in a representative sample of postmenopausal women. Ultrasound Obstet Gynecol 1996;7:322–7.
17. Levine D, Gosink BB, Johnson LA. Change in endometrial thickness in postmenopausal women undergoing hormone replacement therapy. Radiology 1995;197:603–8.
18. Togashi K, Nakai A, Sugimura K. Anatomy and physiology of the female pelvis: MR imaging revisited. J Magn Reson Imaging 2001;13:842–9.
19. Brown MA. MRI of malignant uterine disease. Magn Reson Imaging Clin N Am 2007;455–69.
20. Creasman W. Revised FIGO staging for carcinoma of the endometrium. Int J Gynaecol Obstet 2009; 105(2):109.
21. Larson DM, Connor GP, Broste SK, et al. Prognostic significance of gross myometrial invasion with endometrial cancer. Obstet Gynecol 1996;88(3):394–8.
22. Berman ML. Prognosis and treatment of endometrial cancer. Am J Obstet Gynecol 1980;136(5):679–88.
23. Sala E, Wakely S, Senior E, et al. MRI of malignant neoplasms of the uterine corpus and cervix. AJR Am J Roentgenol 2007;188:1577–87.
24. Odicino F. History of the FIGO cancer staging system. Int J Gynaecol Obstet 2008;101(2):205–10.
25. Beddy P. FIGO staging system for endometrial cancer: added benefits of MR imaging. Radiographics 2012;32:241–54.
26. Morrow CP. Relationship between surgical-pathological risk factors and outcome in clinical stage I and II carcinoma of the endometrium: a Gynecologic Oncology Group study. Gynecol Oncol 1991;40(1):55–65.
27. Yamashita Y. Normal uterus and FIGO stage I endometrial carcinoma: dynamic gadolinium-enhanced MR imaging. Radiology 1993;186(2):495–501.
28. Manfredi R. Local-regional staging of endometrial carcinoma: role of MR imaging in surgical planning. Radiology 2004;231(2):372–8.
29. Beddy P. Evaluation of depth of myometrial invasion and overall staging in endometrial cancer: comparison of diffusion-weighted and dynamic contrast-enhanced MR imaging. Radiology 2012;262:530–7.
30. Koh DM. Diffusion-weighted MRI in the body: applications and challenges in oncology. AJR Am J Roentgenol 2007;188(6):1622–35.

31. Whittaker CS. Diffusion-weighted MR imaging of female pelvic tumors: a pictorial review. Radiographics 2009;29(3):759–74 [discussion: 774–8].
32. Takeuchi M. Diffusion-weighted magnetic resonance imaging of endometrial cancer: differentiation from benign endometrial lesions and preoperative assessment of myometrial invasion. Acta Radiol 2009;50(8):947–53.
33. Rechichi G. Endometrial cancer: correlation of apparent diffusion coefficient with tumor grade, depth of myometrial invasion, and presence of lymph node metastases. AJR Am J Roentgenol 2011;197(1):256–62.
34. Rechichi G. Myometrial invasion in endometrial cancer: diagnostic performance of diffusion-weighted MR imaging at 1.5 T. Eur Radiol 2010;20(3):754–62.
35. Murase E, Outwater EK, Tureck RW. Uterine leiomyomas: histopathologic features, MR imaging findings, differential diagnosis, and treatment. Radiographics 1999;19:1179–97.
36. Tamai K, Koyama T, Saga T, et al. The utility of diffusion-weighted MR imaging for differentiating uterine sarcomas from benign leiomyomas. Eur Radiol 2008;18(4):723–30.
37. Bakir B, Bakan S, Tunaci M, et al. Diffusion-weighted imaging of solid or predominantly solid gynaecological adnexial masses: is it useful in the differential diagnosis? Br J Radiol 2011;84:600–11.
38. Takeuchi M. Hyperintense uterine myometrial masses on T2-weighted magnetic resonance imaging: differentiation with diffusion-weighted magnetic resonance imaging. J Comput Assist Tomogr 2009; 33(6):834–7.
39. Jacobs MA. Comparison between diffusion-weighted imaging, T2-weighted, and postcontrast T1-weighted imaging after MR-guided, high intensity, focused ultrasound treatment of uterine leiomyomata: preliminary results. Med Phys 2010; 37(9):4768–76.
40. Takeuchi M. Susceptibility-weighted MRI of endometrioma: preliminary results. AJR Am J Roentgenol 2008;191:1366–70.
41. Takeuchi M. Adenomyosis usual and unusual manifestations, pitfalls and problem solving imaging technique. Radiographics 2011;31:99–115.
42. Haacke EM, Xu Y, Cheng YC, et al. Susceptibility weighted imaging (SWI). Magn Reson Med 2004; 52:612–8.
43. Okamoto Y. MR imaging of the uterine cervix: imaging-pathologic correlation. Radiographics 2003;23: 425–45.
44. Nakai A. Functional MR imaging of the uterus. Magn Reson Imaging Clin N Am 2008;16:673–84.
45. Naganawa S, Sato C, Kumada H, et al. Apparent diffusion coefficient in cervical cancer of the uterus: comparison with the normal uterine cervix. Eur Radiol 2005;15:71–8.
46. McVeigh PZ. Diffusion weighted MRI in cervical cancer. Eur Radiol 2008;18:1058–64.
47. Somoye G, Vanessa H, Semple S, et al. Early diffusion weighted magnetic resonance imaging can predict survival in women with locally advanced cancer of the cervix treated with combined chemoradiation. Eur Radiol 2012;22(11):2319–27.
48. Boss EA. Post-radiotherapy contrast enhancement changes in fast dynamic MRI of cervical carcinoma. J Magn Reson Imaging 2001;13:600–6.
49. Yamashita Y. Dynamic-contrast enhanced MR imaging of uterine cervical cancer: pharmokocinetic analysis with histopathologic correlation and its importance in predicting the outcome of radiation therapy. Radiology 2000;216:803–9.
50. Balleyguier C. Staging of uterine cervical cancer with MRI: guidelines of the European Society of Urogenital Radiology. Eur Radiol 2011;21(5):1102–10.
51. Umemoto M, Shiota M, Shimono T, et al. Preoperative diagnosis of ovarian tumors, focusing on the solid area based on diagnostic imaging. J Obstet Gynaecol Res 2006;32(2):195–201.
52. Sohaib SA, Sahdev A, Van Trappen P, et al. Characterization of adnexal mass lesions on MR imaging. AJR Am J Roentgenol 2003;180(5):1297–304.
53. Rosai J. Female reproductive system. Ackerman's surgical pathology. 8th edition. St. Louis (MO): 1996.
54. Togashi K, Nishimura K, Kimura I, et al. Endometrial cysts: diagnosis with MR imaging. Radiology 1991; 180:73–8.
55. Kim SH. Unusual causes of tubo-ovarian abscess: CT and MR imaging findings. Radiographics 2004; 24:1575–89.
56. Thomassin-Naggara I, Daraï E, Cuenod CA, et al. Contribution of diffusion-weighted MR imaging for predicting benignity of complex adnexal masses. Eur Radiol 2009;19(6):1544–52.
57. Li W, Zhang W, Wu X. Pelvic inflammatory disease: evaluation of diagnostic accuracy with conventional MR with added diffusion-weighted imaging. Abdom Imaging 2012. DOI:10.1007.
58. Takeshita T. Diffusion-weighted magnetic resonance imaging in tubo-ovarian abscess: a case report. Osaka City Med J 2009;55:109–14.
59. Chang HC. Pearl and pitfalls in diagnosis of ovarian torsion. Radiographics 2008;28:1355–68.
60. Lee EJ, Kwon HC, Joo HJ, et al. Diagnosis of ovarian torsion with color Doppler sonography: depiction of twisted vascular pedicle. J Ultrasound Med 1998; 17(2):83–8.
61. Graif M, Shalev J, Strauss S, et al. Torsion of the ovary: sonographic features. AJR Am J Roentgenol 1984;6:1331–4.
62. Warner BW, Kuhn JC, Barr LL. Conservative management of large ovarian cysts in children: the value of serial pelvic ultrasonography. Surgery 1992;112(4):749–55.

63. Ferlay J, Shin HR, Bray F, et al. GLOBOCAN Cancer incidence and mortality worldwide: IARC CancerBase no. 10. International Agency for Research on Cancer, Lyon. 2008. Available at: http://www.globocan.iarc.fr. Accessed January 11, 2011.
64. Ellenson. Female genital tract. In: Kumar V, Abbas AK, Aster J, et al, editors. Robbins and Cotran pathologic basis of disease. Philadelphia: Elsevier Saunders; 2010. p. 1005–64.
65. Mohagegh P. Imaging strategy for early ovarian cancer: characterization of adnexal masses with conventional and advanced imaging techniques. Radiographics 2012;32:1751–73.
66. Sohaib SA. The role of magnetic resonance imaging and ultrasound in patients with adnexal masses. Clin Radiol 2005;60(3):340–8.
67. Takeuchi M, Matsuzaki K, Nishitani H. Diffusion-weighted magnetic resonance imaging of ovarian tumors: differentiation of benign and malignant solid components of ovarian masses. J Comput Assist Tomogr 2010;34(2):173–6.
68. Thomassin-Naggara I, Marsault C, Bazot M. Dynamic contrast-enhanced MR imaging of ovarian neoplasms: current status and future perspectives. Magn Reson Imaging Clin N Am 2008;16:661–72.
69. Katayama M, Masui T, Kobayashi S, et al. Diffusion-weighted echo planar imaging of ovarian tumors: is it useful to measure apparent diffusion coefficients? J Comput Assist Tomogr 2002;26:250–6.
70. Fujii S, Kakite S, Nishihara K, et al. Diagnostic accuracy of diffusion-weighted imaging in differentiating benign from malignant ovarian lesions. J Magn Reson Imaging 2008;28:1149–56.
71. Low RN, Sebrechts CP, Barone RM, et al. Diffusion-weighted MRI of peritoneal tumors: comparison with conventional MRI and surgical and histopathologic findings— a feasibility study. AJR Am J Roentgenol 2009;193(2):461–70.
72. Kyriazi S, Collins DJ, Messiou C, et al. Metastatic ovarian and primary peritoneal cancer: assessing chemotherapy response with diffusion-weighted MR imaging—value of histogram analysis of apparent diffusion coefficients. Radiology 2011;261: 182–92.
73. Hricak H, Chen M, Coakley FV, et al. Complex adnexal masses: detection and characterization with MR imaging—multivariate analysis. Radiology 2000;214(1):39–46.
74. Jain RK. Determinants of tumor blood flow: a review. Cancer Res 1988;48(10):2641–58.
75. Thomassin-Naggara I, Darai E, Nassar-Slaba J, et al. Value of dynamic enhanced magnetic resonance imaging for distinguishing between ovarian fibroma and subserous uterine leiomyoma. J Comput Assist Tomogr 2007;31(2):236–42.
76. Thomassin-Naggara I. Dynamic-contrast enhanced MR imaging to assess physiologic variations of myometrial perfusion. Eur Radiol 2010;20(4):984–94.